Received: 27 February 2020 | Accepted: 1 May 2020

DOI: 10.1111/gcbb.12717

ORIGINAL RESEARCH

GCB-BIOENERGY BIOPRODUCTS FOR A SUSTAINABLE BIOECONOMY Open Access

WILEY

Resource utilization conditions as biochar of an invasive plant *Spartina alterniflora* in coastal wetlands of China

Huijuan Xia[1] | **Weijing Kong**[1] | **Lusan Liu**[1] | **Hongli Li**[2] | **Kuixuan Lin**[1]

[1]National Engineering Laboratory for Lake Pollution Control and Ecological Restoration, State Environmental Protection Key Laboratory for Lake Pollution Control, State Environmental Protection Scientific Observation and Research Station for Lake Dongtinghu, State Environmental Protection Key Laboratory of Estuarine and Coastal Environment, Chinese Research Academy of Environmental Sciences, Beijing, China

[2]College of Nature Conservation, Beijing Forestry University, Beijing, China

Correspondence
Weijing Kong, Chinese Research Academy of Environmental Sciences, Beijing 100012, China.
Email: kongwj@craes.org.cn

Funding information
National Key R&D Program of China, Grant/Award Number: 2017YFC0505905

Abstract

Converting feedstocks of invasive plants into biochar is a new and cost-effective measure for their control, and benefits for the sustainable development of native ecosystems. *Spartina alterniflora*, an invasive plant widely distributed in coastal wetlands of China, was used to produce biochar. We aimed to analyze how *S. alterniflora* biochar properties changed with desalination of feedstocks, pyrolysis temperature, and residence time. Results showed that desalting feedstocks increased biochar pH, stability, porosity, and surface area, but diminished biochar yield and polarity. Pyrolysis temperature positively affected biochar pH, surface area, and pore volume, while it had negative effects on biochar yield, oxygen and hydrogen contents, hydrogen/carbon and oxygen/carbon ratios, pore size, and function groups. However, residence time of pyrolysis had slight effects on biochar properties. The results are valuable for optimizing pyrolysis temperature and pretreatment measure of feedstocks, to tune *S. alterniflora* biochar properties for specific environmental usage.

KEYWORDS

biochar, desalination, invasive plants, pyrolysis temperature, resource utilization, *Spartina alterniflora*

1 | INTRODUCTION

Invasive plants have caused serious damages to native biodiversity, local habitats, and even public health and economy by outcompeting with native plants and rapidly expanding (Liao, Gao, & Fang, 2013; Pimentel, 2002). Various clearing measures, such as clipping, pulling, digging, and applying herbicides, are widely used to control invasive plants (Shimeta, Saint, Verspaandonk, Nugegoda, & Howe, 2016; Tang et al., 2009; Waryszak, Lenz, Leishman, & Downey, 2018). Although some successes have been achieved, these measures always bring high cost, and chemical measures may impose damages to native species (Liao et al., 2013; Simmons et al., 2007). Furthermore, physical clearing measures leave amounts of plant wastes, and lead to serious environmental pollution (de Lange, Stafford, Forsyth, & le Maitre, 2012). Utilizing these wastes as a kind of resource presents a promising and sustainable strategy for management of invasive plants (Liao et al., 2013).

As an environmentally benign material, biochar attracts increasing attentions for the resource utilization of invasive plant wastes by transforming them into valued materials (Liao et al., 2013). Biochar is produced by pyrolyzing organic matters at high temperature with limited or no oxygen supply (Ahmad et al., 2014; Moore et al., 2018), and has promising use in carbon storage, environmental remediation, soil amelioration, and agricultural productivity improvement (Oliveira et al., 2017; Xu et al., 2017; Zhang et al., 2017). These environmental applications of biochar

are attributed to its high organic C contents, large specific surface area and porosity, and diverse functional groups (Oliveira et al., 2017).

Multiple carbonaceous feedstocks were used to produce biochar, such as agricultural residues (Vu et al., 2017; Zhao et al., 2018), forest residues (Fernandes et al., 2019; Mohan et al., 2007), manures (Wang & Liu, 2018; Wei et al., 2018), activated sludge (Stefaniuk, Tsang, Ok, & Oleszczuk, 2018; Waqas, Khan, Qing, Reid, & Chao, 2014), and waste biomass (de Jesus, da Cunha, Cardoso, Mangrich, & Romão, 2017; Nie et al., 2018). Nowadays, invasive plants have also attracted attentions to produce biochar due to their wide distribution and high biomass, for example, Brazilian Pepper and Air Potato in southeastern United States (Liao et al., 2013), *Sicyos angulatus* in Korea (Rajapaksha et al., 2014; Vithanage et al., 2014), and *Spartina alterniflora* in China (Li & Wang, 2009; Li et al., 2013). These biochars showed effectiveness in removing pollutants from aqueous solutions or agricultural soils.

S. alterniflora, a rhizomatous plant native to Northern American coast, was introduced to China in 1979 for protecting beach and promoting siltation (Lu & Zhang, 2013; Zheng et al., 2016). It distributes widely in Chinese coastal wetlands nowadays, and difficult to clear because of its strong adaptation and propagation ability (Li et al., 2009; Wang et al., 2008). The annual biomass of *S. alterniflora* in China is estimated to be higher than 2×10^6 t (Lu & Zhang, 2013), presenting a promising and sustainable feedstock for biochar. However, *S. alterniflora* is a salt marsh plant with high salt contents (Qin et al., 2016). The produced biochar may present risks during its utilization in environmental remediation, thus desalination treatment for diminishing salt contents in feedstocks is needed to reduce potential environmental risks. Although biochar properties vary with feedstock types (Ahmad et al., 2014; Li, Harris, Anandhi, & Chen, 2019; Ronsse, van Hecke, Dickinson, & Prins, 2013), whether desalination treatment of the same feedstock affects biochar properties is not well known.

Biochar properties are affected not only by feedstock types but also by pyrolysis conditions such as pyrolysis temperature and residence time (Zhao, Ta, & Wang, 2017; Zhou et al., 2018). Characterizing *S. alterniflora* biochar that pyrolyzed under different conditions is critical to produce biochar with specific properties for environmental usage. Efforts have been taken to produce *S. alterniflora* biochar at 700°C and 400°C for 2 hr, and the biochar was used to remove heavy metal (e.g., copper and lead) from water (Li & Wang, 2009; Li et al., 2013). However, less data can be acquired from previous studies to fully understand *S. alterniflora* biochar properties.

In the study, untreated and desalted *S. alterniflora* feedstocks were pyrolyzed under different temperature and residence time to produce biochar. Biochar physical (e.g., yield), chemical (e.g., pH and elemental composition), and surface properties (e.g., surface morphology, surface area, porosity, and functional groups) were examined. We aimed to (a) reveal whether and how desalination treatment of feedstocks affected biochar properties, (b) analyze how *S. alterniflora* biochar properties changed with pyrolysis temperature and residence time. These results help identify the optimal pyrolysis conditions to get specific biochar during resource utilization of *S. alterniflora*, and provide data for environmental application of biochar.

2 | MATERIALS AND METHODS

2.1 | Feedstock preparation

S. alterniflora was collected from the Yellow River estuary in Dongying city, China. The collected *S. alterniflora* feedstocks were washed using deionized water to remove surface contaminations. Half of feedstock materials were soaked in deionized water to get the desalted feedstocks. Multiple experiments determined that desalting feedstocks for 3 hr in deionized water with the feedstock–water ratio of 1 g:25 ml can reduce salt contents in feedstocks to a normal level below 1.84% (Figure S1). The desalted and untreated feedstocks were chopped into short segments (<5 mm) and air-dried for 7 days. The feedstock segments were dried in an oven for 24 hr under 105°C, and sealed in plastic bags.

2.2 | Pyrolysis method for biochar

To avoid air flowing into ceramic crucibles and create an oxygen-limited atmosphere, the oven-dried feedstocks were tightly packed into ceramic crucibles, which were then covered by two layers of aluminum foil. The crucibles filled with feedstocks were pyrolyzed under high temperature in muffle furnace (SX-G16103) with limited oxygen supply. After the temperature in muffle furnace decreased to 25°C, the crucibles were taken out. The produced biochar was sealed in plastic bags and marked feedstock type (desalted or untreated), pyrolysis temperature, and residence time.

Our previous thermogravimetric analysis showed that *S. alterniflora* feedstocks were not thermally stable due to the sharp mass loss as increasing temperature up to 350°C (Figure S2). While the feedstocks presented stable mass loss at temperature above 350°C, and followed by slight mass loss above 650°C. Thus, to reveal the dynamics of biochar properties with pyrolysis temperature, feedstocks were pyrolyzed at temperature of 350°C–650°C in 50°C intervals for 2 hr, which is a widely used residence time. Biochar produced from *S. alterniflora* at 450°C had higher adsorption capacity (Qiu, Zhou, Han, & Zhang, 2018). Feedstocks were pyrolyzed at 450°C for 0.5, 1, 2, and 3 hr based on previous studies to reveal the dynamics of biochar properties with residence time

(Chandra & Bhattacharya, 2019; Kong, Gao, Zhou, Zhao, & Sun, 2018; Shaaban et al., 2014). The temperature in muffle furnace was raised at a rate of 5°C/min.

2.3 | Analysis of biochar properties

The yield, pH, elemental composition, surface morphology, surface area, porosity, and functional group of *S. alterniflora* biochar were measured.

The weight ratio of biochar to feedstock was used to represent biochar yield (Chandra & Bhattacharya, 2019). The pH was measured using pH probe (SL1000, Hach) at the biochar-deionized water ratio of 1 g:20 ml after shaking for 1 hr and standing for 5 min (Ahmad et al., 2018). Elemental composition (C, H, O, and N) was measured with elemental analyzer (Vario EL cube, Elementar). Surface morphology was obtained using scanning electron microscopy (SEM, JSM-6480LV, Hitachi). The nitrogen gas adsorption/desorption isotherms were analyzed at −196°C with automatic instruments (ASAP 2460, Micromeritics). The pore size and volume were calculated using Barrett–Joyner–Halenda equation, and the surface area was calculated using Brunauer–Emmet–Teller equation (Zhao et al., 2018). Functional groups were identified using Fourier transformed infrared spectroscopy (FTIR; Zhao et al., 2018). FTIR spectra were obtained from 400 to 4,000 cm^{-1} in 4 cm^{-1} intervals with an FTIR spectrometer (Nicolet 6700, Thermo Fisher).

2.4 | Statistical analysis

SPSS Statistics software version 17.0 (SPSS Inc.) was used to perform the statistical analysis of the data. Basic analysis of mean, minimum, and maximum was conducted for biochar properties. The correlations between biochar properties (yield and pH) and pyrolysis (temperature and residence time) were fitted using the Curve Estimation procedure.

3 | RESULTS

3.1 | Biochar yield and pH

S. alterniflora biomass experienced a weight loss near 60% at 350°C, and biochar yield ranged from 23.82% in 650°C to 42.39% in 350°C (Figure 1a). *S. alterniflora* biochar yield showed a steady decreasing trend as increasing temperature from 350°C to 650°C. The yield of biochar produced from untreated and desalted feedstocks decreased 30% and 40% as increasing temperature up to 650°C, respectively (Figure 1a). The yield of biochar produced from untreated and desalted feedstocks decreased only 3.64% and 3.45% with residence time increased from 0.5 to 3 hr, respectively (Figure 1b). The yield of biochar produced from untreated *S. alterniflora* was higher than that produced from desalted feedstocks (Figure 1).

S. alterniflora biochar was strongly alkaline with pH ranging from 10.04 to 11.46 (Figure 2a). The pH showed a sharp increase as increasing temperature from 350°C to 500°C, and became steady above 500°C with slight decline from 600°C to 650°C (Figure 2a). The maximum pH of *S. alterniflora* biochar occurred at 500°C, 11.46, and 11.04 for biochar produced from desalted and untreated feedstocks, respectively. As residence time of pyrolysis increased from 0.5 to 3 hr, the pH only increased 0.21 and 0.24 units for biochar produced from desalted and untreated feedstocks, respectively (Figure 2b).

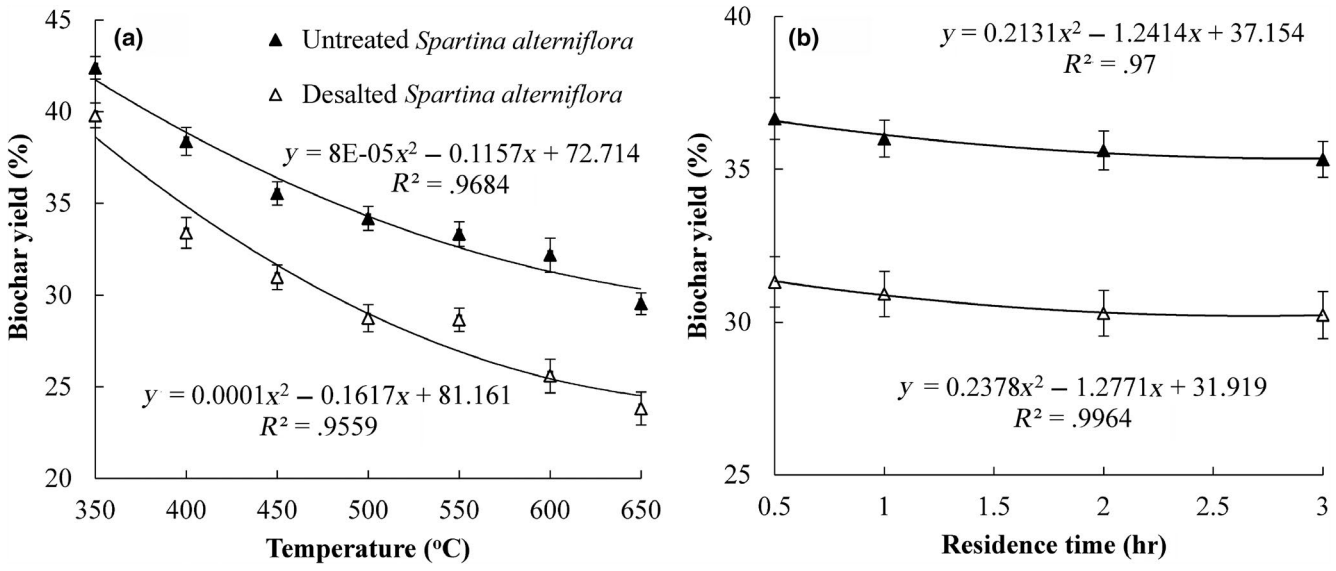

FIGURE 1 Changes in biochar yield with pyrolysis temperature (a) and residence time (b)

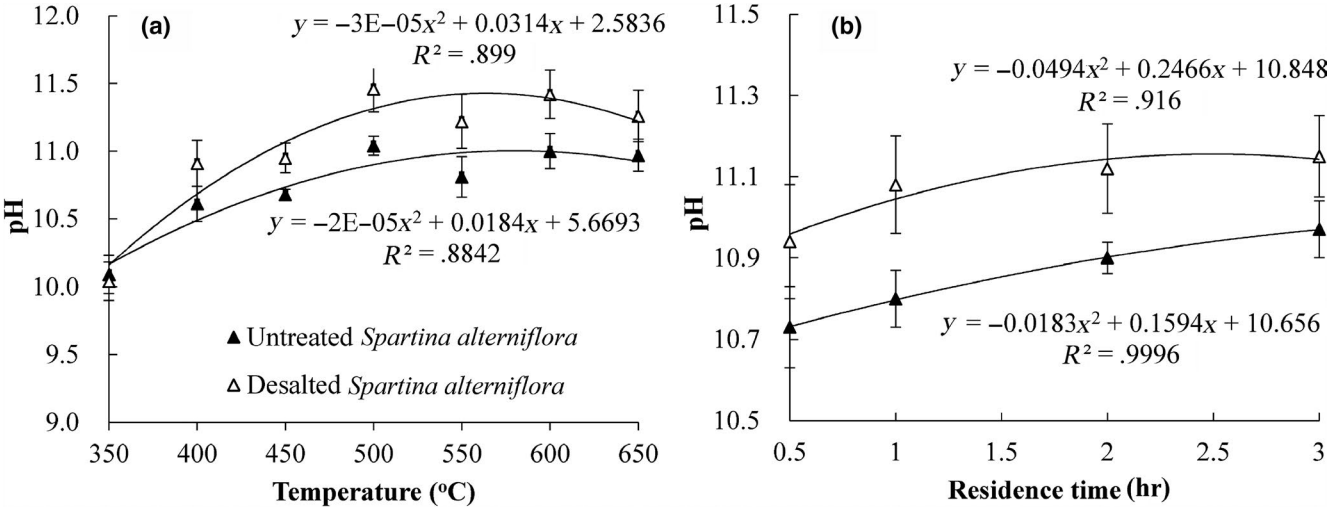

FIGURE 2 Changes in biochar pH with pyrolysis temperature (a) and residence time (b)

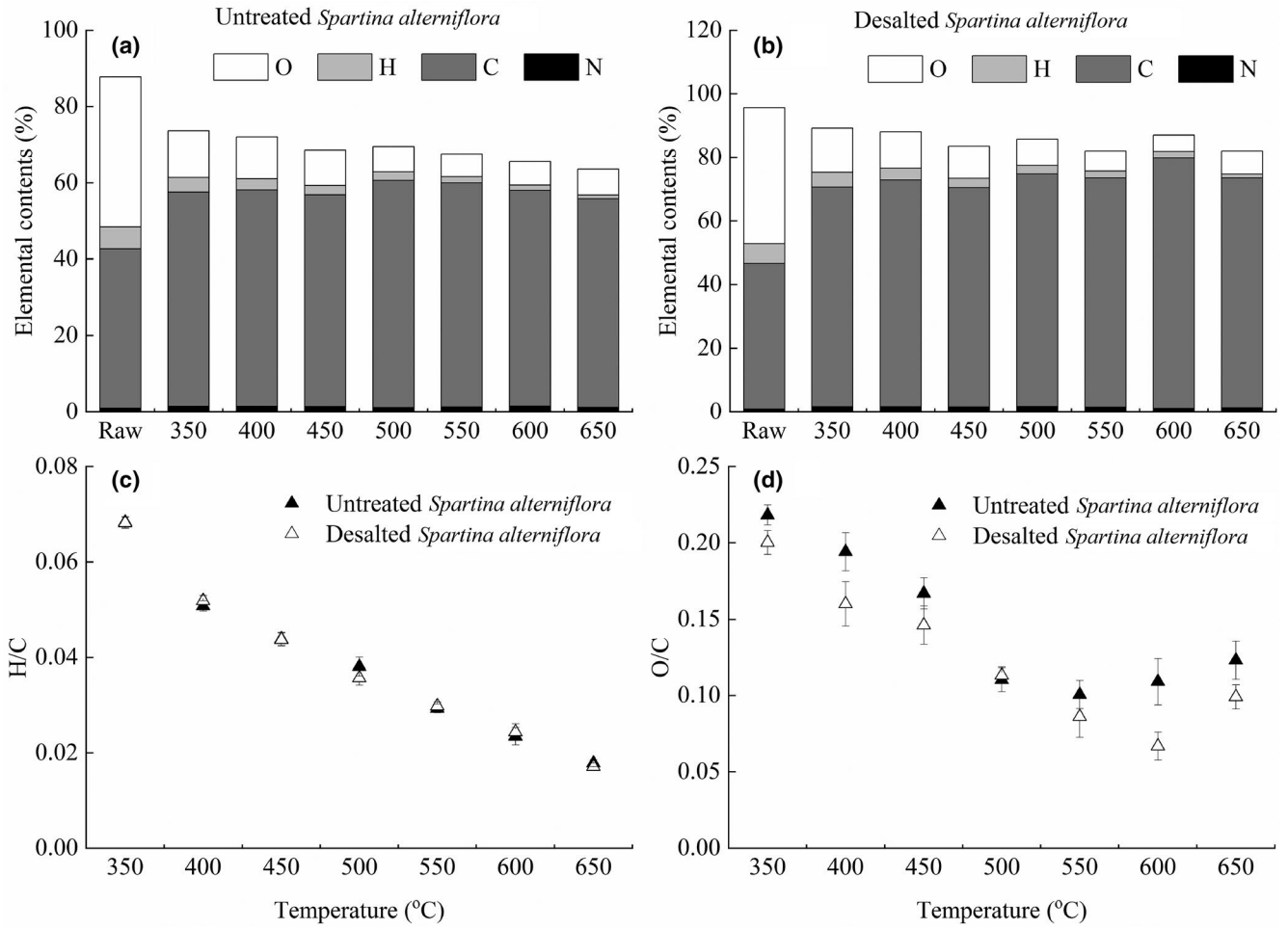

FIGURE 3 Changes in biochar elemental contents (a, b), H/C ratio (c), and O/C ratio (d) with pyrolysis temperature. C, carbon; H, hydrogen; O, oxygen

3.2 | Elemental composition

Pyrolysis of raw feedstocks decreased O and H contents, and increased C and N contents (Figure 3a,b). Carbonization during pyrolysis induced the increase of C contents in *S. alterniflora* biochar, although the increasing trend was observed with slight fluctuation. The O and H contents declined as increasing pyrolysis temperature, and N contents in *S. alterniflora* biochar showed

no significant changing trend with pyrolysis temperature (Figure 3a,b).

The H/C and O/C ratios in *S. alterniflora* biochar decreased as increasing temperature (Figure 3c,d). However, the O/C ratio in biochar produced from desalted feedstocks increased as increasing temperature from 600°C to 650°C, and that of biochar produced from untreated feedstocks increased as increasing temperature from 550°C to 650°C. Although O/C ratio increased at high temperature, they were still lower at high temperature of 500°C–650°C than that at low temperature of 350°C–450°C (Figure 3d).

The C, H, O, and N contents in biochar showed no significant changes with different residence time (Figure 4a,b). The H/C and O/C ratios showed slight decreasing trends as residence time increased from 0.5 to 3 hr (Figure 4c,d).

The C, H, O, and N contents in biochar produced from untreated *S. alterniflora* were lower than that produced from desalted feedstocks (Figures 3 and 4). The O/C ratio of biochar produced from desalted *S. alterniflora* generally was lower than that produced from untreated feedstocks (Figures 3 and 4). The H/C ratios showed no significant difference between biochar produced from desalted and untreated feedstocks (Figures 3 and 4).

3.3 | Surface morphology

Raw feedstocks had little pore, and pores appeared in biochar as increasing pyrolysis temperature (Figure 5). *S. alterniflora* biochar pyrolyzed at 350°C showed visible tube-like pore structures, and the pore wall of tube-like structures became thinner and even collapsed as increasing temperature. Micropores occurred on the pore wall and micropores quantity increased as increasing temperature (Figure 5). Contrasting with pyrolysis temperature, residence time had no significant effects on biochar surface morphology (Figure 6).

The pore shape of biochar produced from desalted *S. alterniflora* was more irregular than that produced from untreated feedstocks, and the quantity of meso- and micropores in desalted biochar was higher than untreated biochar

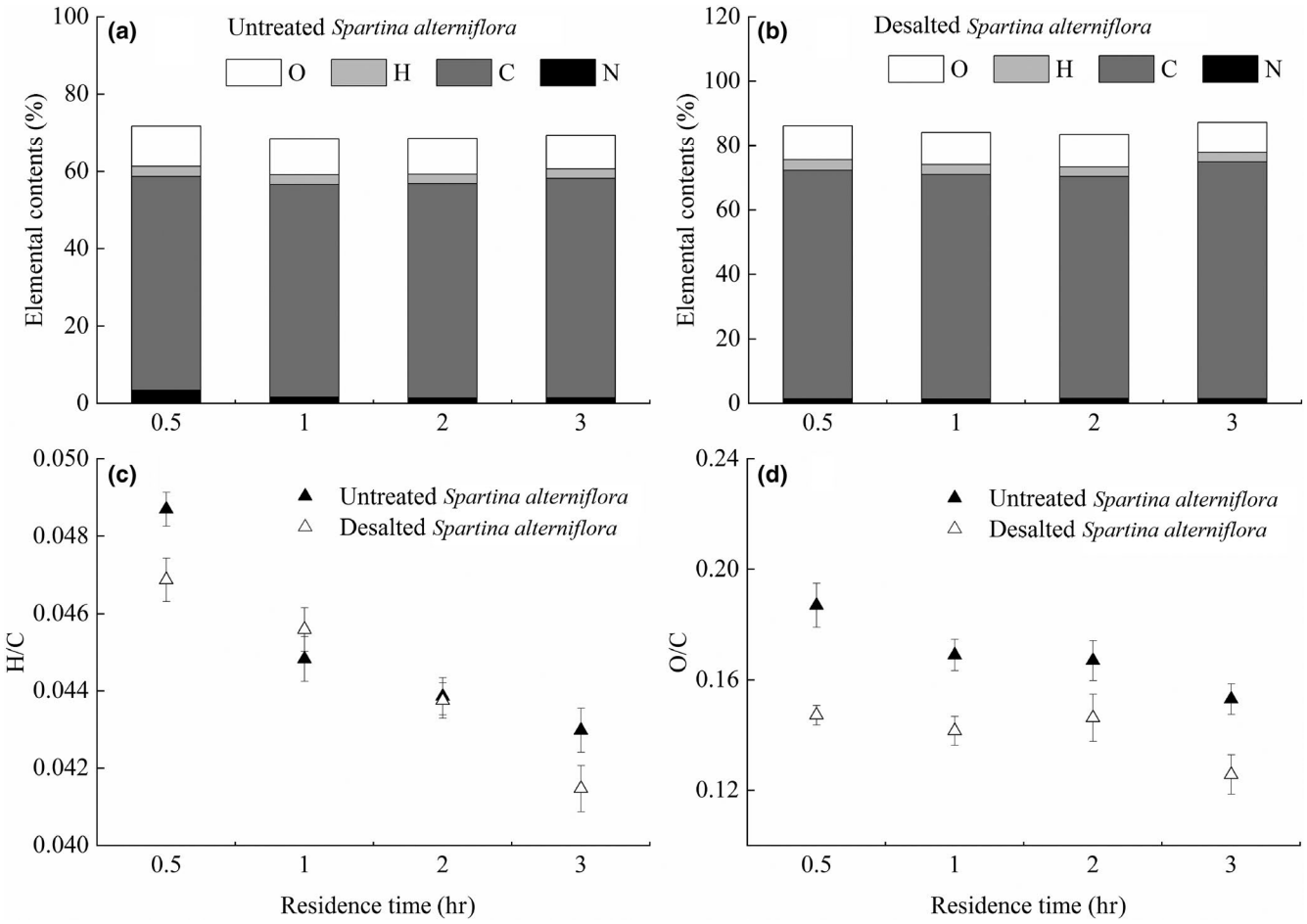

FIGURE 4 Changes in biochar elemental contents (a, b), H/C ratio (c), and O/C ratio (d) with residence time. C, carbon; H, hydrogen; O, oxygen

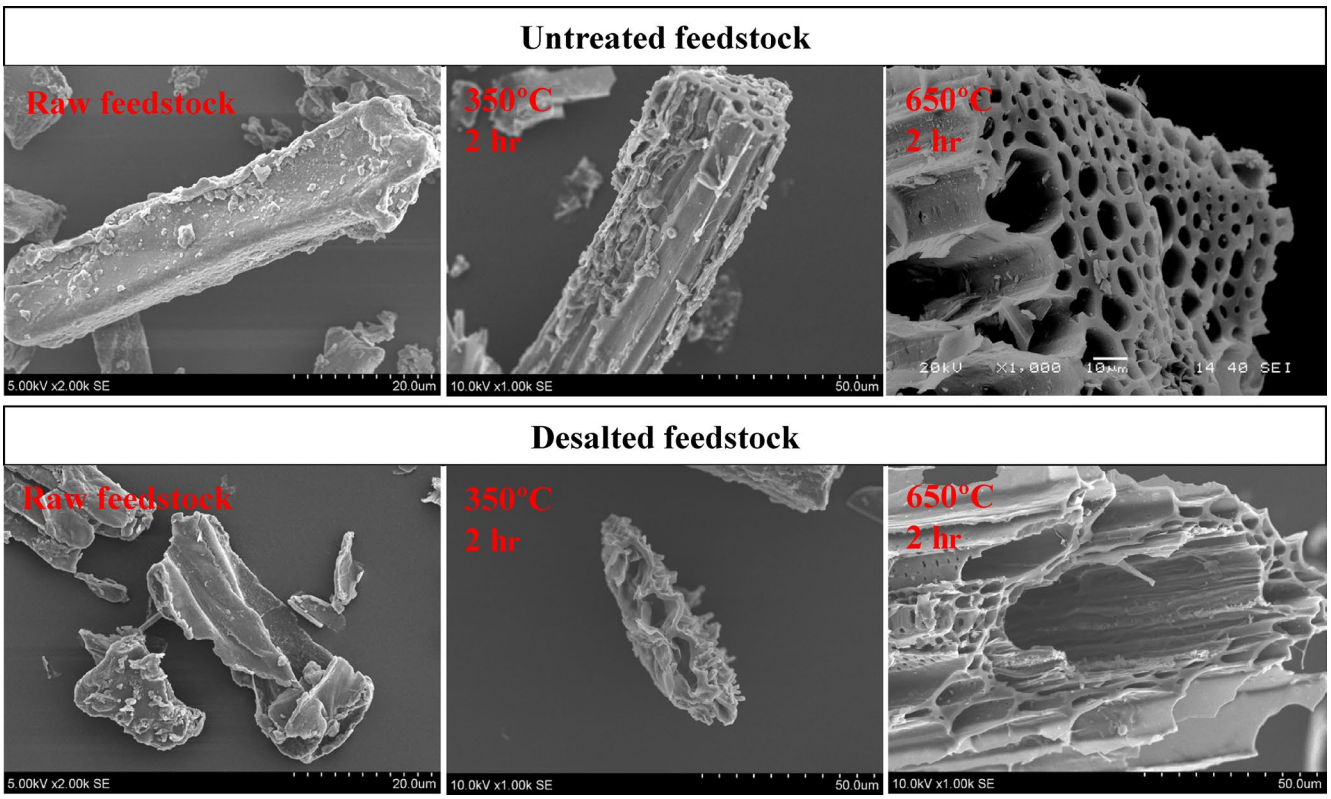

FIGURE 5 SEM images of raw feedstocks and biochar produced at different temperatures (only images at 350°C and 650°C were shown). SEM, scanning electron microscopy

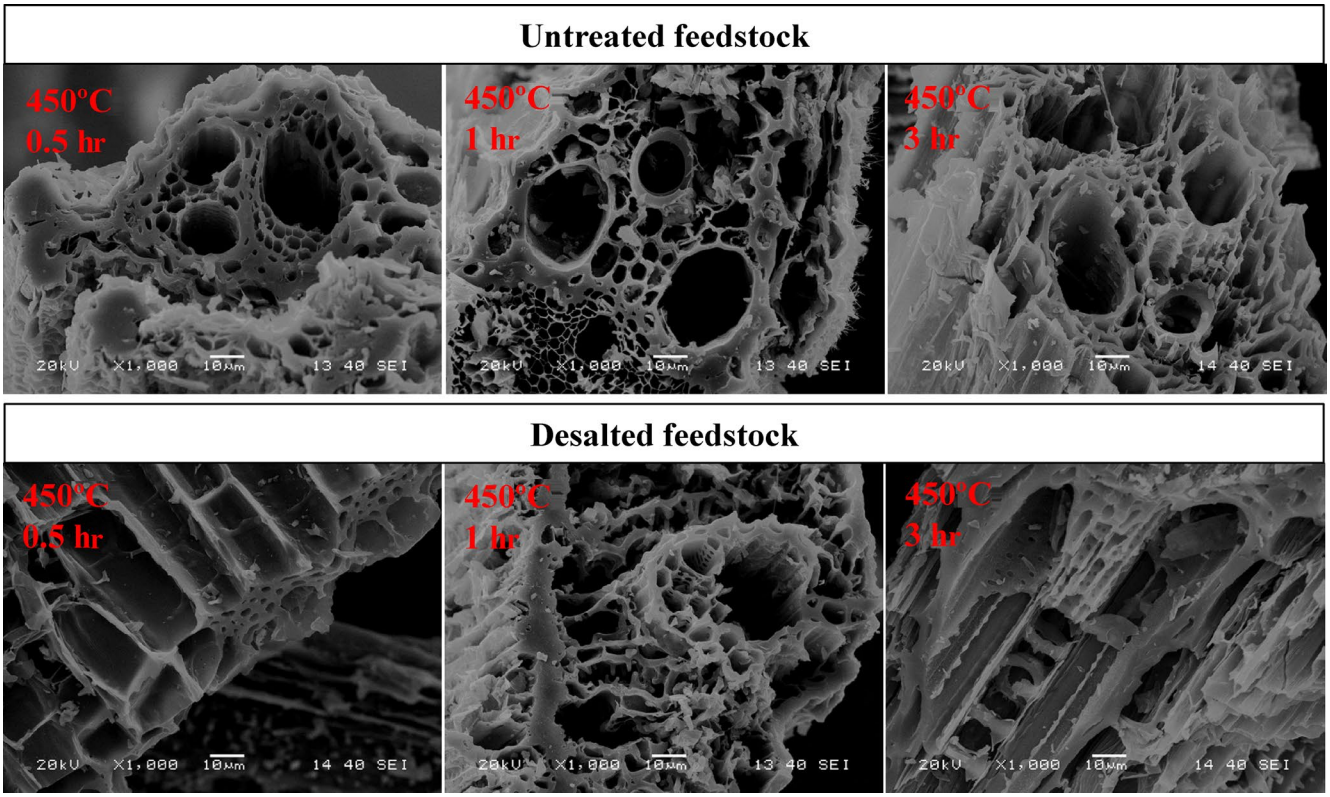

FIGURE 6 SEM images of *Spartina alterniflora* biochar produced at residence time of 0.5, 1, and 3 hr. SEM, scanning electron microscopy

(Figures 5 and 6). The difference of SEM images was consistent with results of biochar surface area and porosity (Figure 7).

3.4 | Surface area and porosity

Biochar surface area and porosity significantly varied with pyrolysis temperature in the study, but showed no apparent changing trends with residence time (Figure 7). Surface area and pore volume of *S. alterniflora* biochar were relatively low, and showed no significant changing trends with temperature increased from 350°C to 500°C (Figure 7). Significant increases of surface area, mesopore volume, and total pore volume were found as increasing temperature from 550°C to 650°C (Figure 7).

Average pore diameter of biochar produced from untreated feedstocks decreased as increasing temperature, and presented a sharp decrease from 450°C to 500°C (Figure 7). Average pore diameter of biochar produced from desalted feedstocks showed a changing trend of single peak curve as increasing temperature, and the peak occurred at 450°C (Figure 7). The surface area and porosity of biochar produced from desalted *S. alterniflora* were higher than that produced from untreated feedstocks (Figure 7).

3.5 | Functional groups

The FTIR spectra showed changes in functional groups with various pyrolysis temperature and residence time (Figure 8). In the given spectra, the peak at 3,400 cm^{-1} was linked with -OH group. The peaks at 2,923 and 1,435 cm^{-1} were linked with aliphatic -CH_x stretching. The peak at 1,574 cm^{-1} corresponded to the presence of C=C stretching. The peak at band range of 1,110–1,114 cm^{-1} was linked with ether C-O-C group. The peak at 875 cm^{-1} was linked with the C-H group.

The intensity and diversity of functional groups on *S. alterniflora* biochar surface decreased as increasing pyrolysis temperature. At 650°C, there were almost no functional groups on biochar surface. The intensity of the -OH group was weak, and became negligible at temperature above 500°C. The -CH_x group at 2,923 cm^{-1} only observed

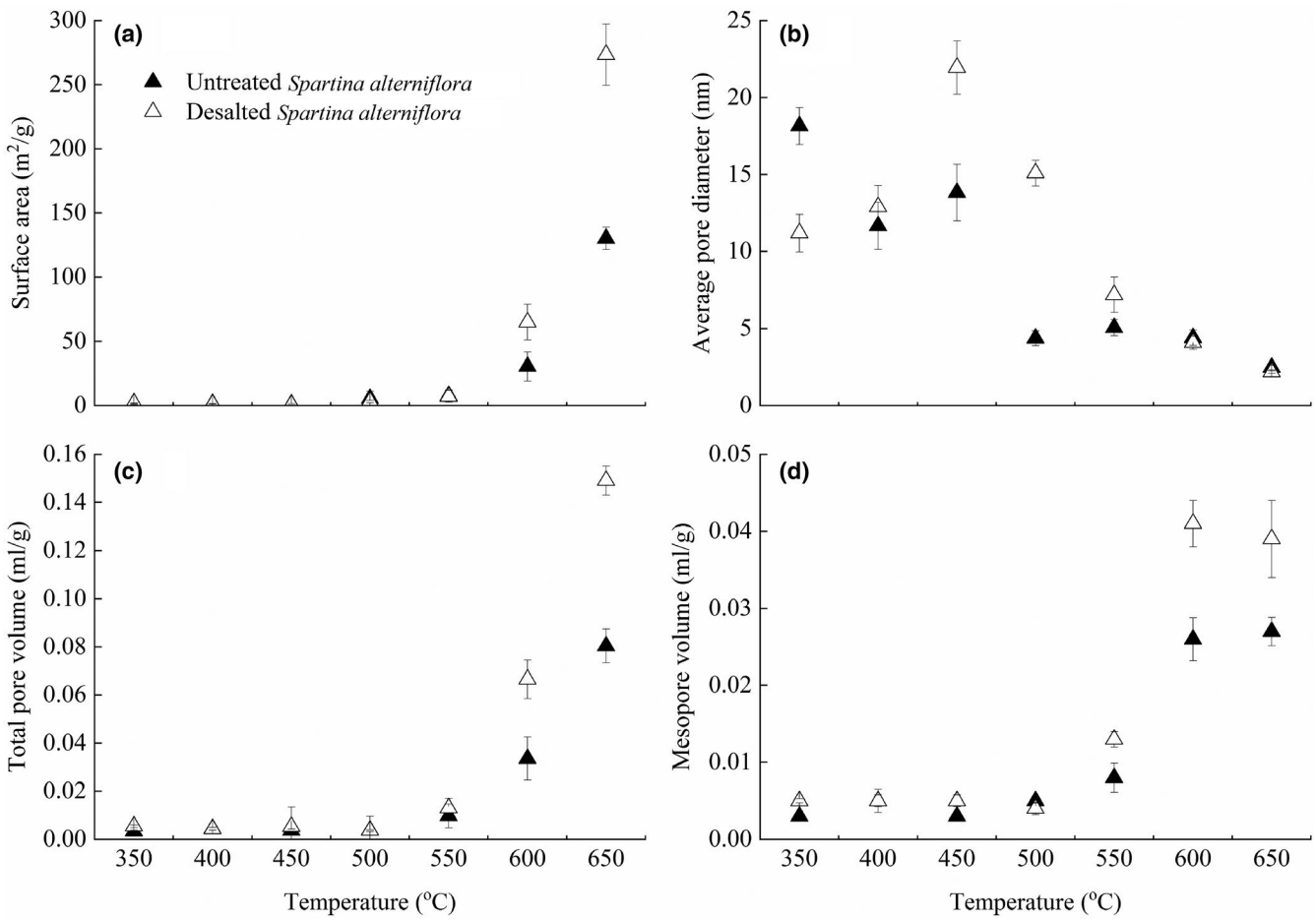

FIGURE 7 Changes in biochar surface area (a), average pore diameter (b), total pore volume (c), and mesopore volume (d) with pyrolysis temperature

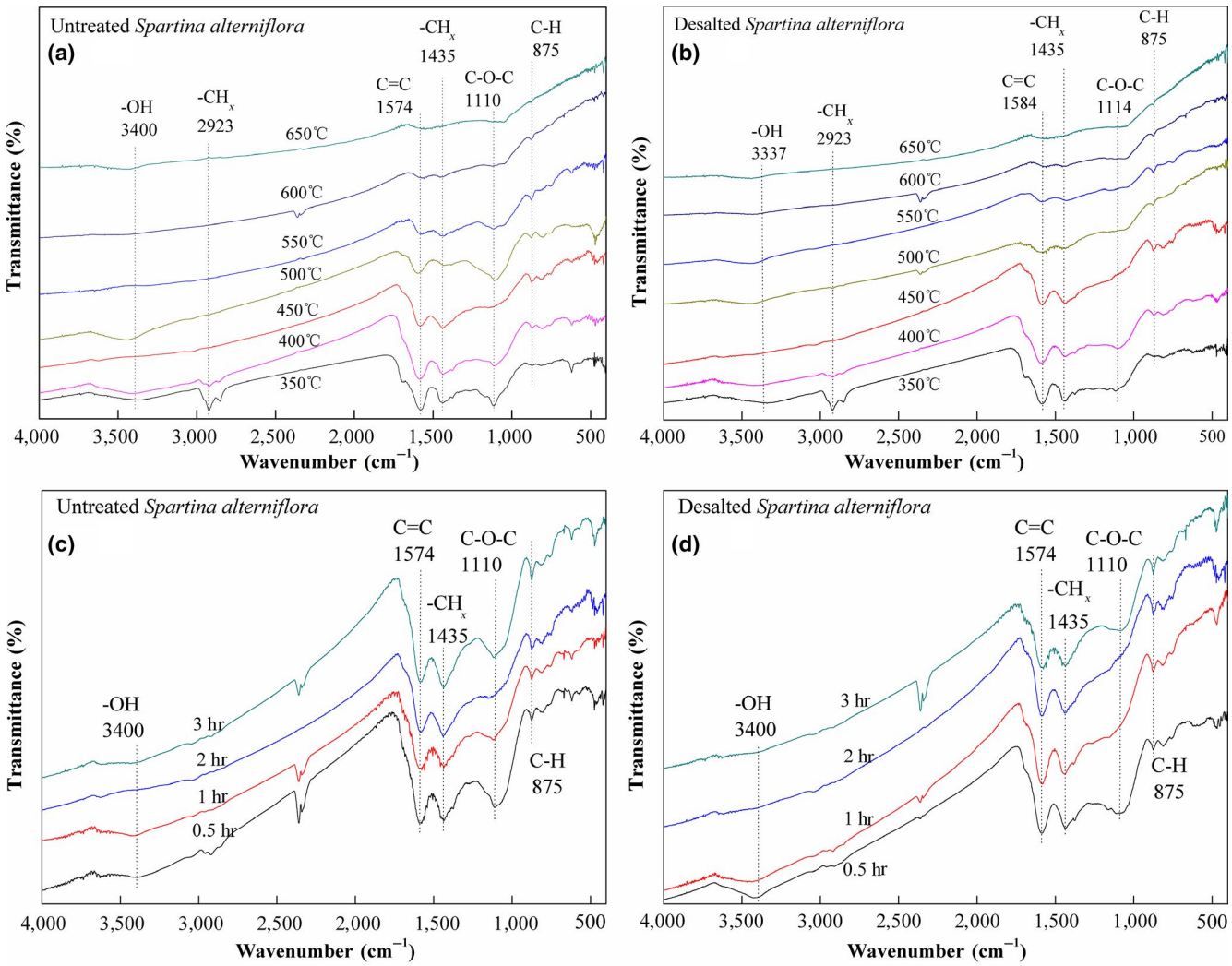

FIGURE 8 Changes in biochar functional groups with pyrolysis temperature (a, b) and residence time (c, d)

at temperature of 350°C and 400°C. The intensity of the C=C group was higher at temperature below 450°C, and declined at temperature above 450°C. Maximum intensity of the C-O-C group for biochar produced from untreated feedstocks was observed at 500°C. However, the C-O-C group for biochar produced from desalted feedstocks only observed at 350°C. The intensity of the C-H group became negligible at 650°C (Figure 8a,b).

Residence time showed no influence on the intensities of C=C, -CH_x, and C-H groups. The intensity of the -OH group was weak, and decreased as residence time increased from 0.5 to 3 hr. While the intensity of the C-O-C group decreased as residence time increased from 0.5 to 2 hr, and increased at a residence time of 3 hr (Figure 8c,d).

Except the C-O-C group, the intensity and diversity of the other functional groups had no significant difference between biochar produced from desalted and untreated *S. alterniflora*. The intensity of the C-O-C group in biochar produced from untreated *S. alterniflora* was higher than that produced from desalted feedstocks (Figure 8).

4 | DISCUSSION

4.1 | Effects of pyrolysis conditions and desalination on biochar yield and pH

Biochar yield rapidly declined as increasing temperature at initial pyrolysis stage, and followed by steady decline (Keiluweit, Nico, Johnson, & Kleber, 2010; Zhao et al., 2018). The rapid decline of *S. alterniflora* biochar yield as increasing temperature was attributed to the removal of water and labile volatile matters from feedstocks (Zhao et al., 2018). The steady decreasing trend of *S. alterniflora* biochar yield as increasing temperature was linked with the dehydration and thermal decomposition of cellulose and lignin (Chandra & Bhattacharya, 2019). Biochar yield slightly decreased as increasing residence time, which indicated the carbonization of *S. alterniflora* was almost completed in a short residence time. Mineral matters played catalytic roles in biochar formation (Raveendran, Ganesh, & Khilar, 1995). Desalination of

feedstocks reduced *S. alterniflora* biochar yield due to the reduction of alkali metals.

The pH is one crucial factor determining the interactions between biochar and polar pollutants (Oliveira et al., 2017). High pH provided more negative surface charge and increased the electrostatic interactions with pollutants, while low pH increased the π-electron donor–acceptor interactions and improved H-bonding for pollutants (Oliveira et al., 2017). Changes in biochar pH were attributed to the decomposition of organic and inorganic components and the formation of alkaline ash (Shinogi & Kanri, 2003). Similar to the changing trends of biochar alkalinity produced from canola, soybean, and peanut straws (Yuan, Xu, & Zhang, 2011), *S. alterniflora* biochar pH showed a sharp increase as increasing temperature from 350°C to 500°C. Biochar pH remained almost constant at high temperature due to the constant contents of ash (Shinogi & Kanri, 2003).

Four categories of biochar alkalinity have been proposed, that is, surface functional group, soluble organic compound, carbonate, and inorganic alkali salt (Fidel, Laird, Thompson, & Lawrinenko, 2017; Shi, Li, Ni, & Xu, 2019). The inorganic alkali salt was separated from feedstocks at pyrolysis temperature over 300°C, and thus increased biochar pH (Cao & Harris, 2010). Although alkali metals (e.g., Na^+, Mg^{2+}, and K^+) were leached from feedstocks by desalination, the pH of biochar derived from desalted *S. alterniflora* was higher than that of untreated feedstocks. In addition, the diversity and intensity functional groups had no significant difference between the two types of biochar. Therefore, the concentrations of soluble organic compound and carbonate in biochar were probably the main causes of *S. alterniflora* biochar alkalinity.

4.2 | Effects of pyrolysis conditions and desalination on elemental composition

The O and H contents declined due to deoxygenation and dehydration of feedstocks as increasing pyrolysis temperature (Li et al., 2015). The N contents in biochar were always affected by feedstock type instead of pyrolysis conditions (Zhao et al., 2018); thus, N contents in *S. alterniflora* biochar showed no significant changing trend with pyrolysis temperature.

The H/C and O/C ratios indicate biochar aromaticity and polarity, respectively (Cao et al., 2019; Tang et al., 2019). The lower H/C and O/C ratios indicated biochar pyrolyzed at higher temperature were more aromatic and less polar, which makes it more stable in environments (Leng & Huang, 2018; Wang, Li, Li, Yu, & Wang, 2019; Zhao et al., 2018). At lower temperature, high O/C ratio indicated more O-containing functional groups appeared in biochar surface, and high H/C ratio indicated more H-C bonds appeared in forms of biodegradable organic matters, which is available for plants and microorganisms (Chandra & Bhattacharya, 2019).

Most of metal salts were deposited in biochar during pyrolysis process, thus desalination reduced C, H, O, and N contents in *S. alterniflora* biochar. The low O/C ratio demonstrated low polarity and high stability of biochar produced from desalted *S. alterniflora* (Zhao et al., 2018).

4.3 | Effects of pyrolysis conditions and desalination on surface morphology, surface area, and porosity

S. alterniflora biochar pyrolyzed at 350°C showed visible tube-like pore structures, which were attributed to the carbonaceous skeleton of feedstocks (Zhang, Liu, & Liu, 2015). As increasing temperature, the pore wall of tube-like structures became thinner and even collapsed due to the destruction of cell structures in feedstocks, which improved biochar porosity. The increase of biochar porosity as increasing temperature was conducive to the diffusion of substances into biochar inner, and provided more interfaces for pollutant adsorption and colonization of soil microorganisms (Chandra & Bhattacharya, 2019; Tan, Sun, Xu, Wang, & Xu, 2016).

The increase of surface area from 300°C to 500°C was attributed to the decomposition of cellulose, which induced the appearance of amorphous carbon structure and micropore as shown by SEM images (Shen et al., 2019). Significant increases of surface area, mesopore volume, and total pore volume from 550°C to 650°C were attributed to the degradation of lignin and release of hydrogen and methane (Taskin et al., 2019; Zhao et al., 2017). Low average pore diameter at high temperature (>500°C) was attributed to the formation of meso- and micropores (Shen et al., 2019).

The residence time and condensation of volatiles in biochar pores can be reduced by demineralization, which increase the amount and rate of volatiles release (Raveendran et al., 1995). Desalination treatment of feedstocks improved the surface area and porosity of *S. alterniflora* biochar. The higher surface area and porosity of biochar produced from desalted *S. alterniflora* indicated their higher adsorption capacity, because larger surface area and richer pore structures provide more opportunity for pollutants adsorption in biochar (Jiang, Lin, & Mbog, 2018).

4.4 | Effects of pyrolysis conditions and desalination on functional groups

The -OH group indicated the occurrence of H-bonding interactions in biochar (Li et al., 2013). The decrease of

-OH group with increasing temperature was attributed to the dehydration of feedstocks (Chen, Yang, Wang, Zhang, & Chen, 2012; Zhao et al., 2017). The C = C group appeared in forms of aromatic hydrocarbons (Chandra & Bhattacharya, 2019). The C = C group intensity declined at temperature above 450°C due to the condensation of aromatic compounds (Li et al., 2017; Shen et al., 2019). The C-O-C group is one of the O-containing functional groups (Cui, Hao, Zhang, He, & Yang, 2016). The intensity of C-O-C group was changed by desalination, which was linked with the different forms of oxygen in desalted and untreated *S. alterniflora* that were converted to carbon chains containing C-O bonds during pyrolysis process (Wang et al., 2019). The C-H group appeared in form of aromatic ring and heteroaromatic compounds, and aromatic ring provides π-electrons to bond inorganic pollutants (Wang et al., 2019).

5 | CONCLUSIONS

S. alterniflora, an invasive plant in Chinese coastal wetlands, was pyrolyzed to produce biochar. Pyrolysis temperature and desalination treatment of feedstocks affected biochar properties. *S. alterniflora* biochar with high alkalinity, stability, surface area, and porosity can be achieved at pyrolysis temperature above 550°C. However, *S. alterniflora* biochar with diverse functional groups can be achieved at temperature below 500°C. Reducing metal salt contents in feedstocks improved the stability, surface area, and porosity of *S. alterniflora* biochar. The above pyrolysis parameters can be used by other researchers and managers to produce biochar with specific properties for environmental usage.

ACKNOWLEDGEMENTS

This work was supported by the National Key R&D Program of China (Grant No. 2017YFC0505905).

DATA AVAILABILITY STATEMENT

Research data are not shared.

ORCID

Huijuan Xia https://orcid.org/0000-0001-9530-5007

REFERENCES

Ahmad, M., Rajapaksha, A. U., Lim, J. E., Zhang, M., Bolan, N., Mohan, D., … Ok, Y. S. (2014). Biochar as a sorbent for contaminant management in soil and water: A review. *Chemosphere*, *99*, 19–33. https://doi.org/10.1016/j.chemosphere.2013.10.071

Ahmad, Z., Gao, B., Mosa, A., Yu, H., Yin, X., Bashir, A., … Wang, S. (2018). Removal of Cu(II), Cd(II) and Pb(II) ions from aqueous solutions by biochars derived from potassium-rich biomass. *Journal of Cleaner Production*, *180*(10), 437–449. https://doi.org/10.1016/j.jclepro.2018.01.133

Cao, X., & Harris, W. (2010). Properties of dairy-manure-derived biochar pertinent to its potential use in remediation. *Bioresource Technology*, *101*(14), 5222–5228. https://doi.org/10.1016/j.biortech.2010.02.052

Cao, Y., Shen, G., Zhang, Y., Gao, C., Li, Y., Zhang, P., … Han, L. (2019). Impacts of carbonization temperature on the Pb(II) adsorption by wheat straw-derived biochar and related mechanism. *Science of the Total Environment*, *692*(20), 479–489. https://doi.org/10.1016/j.scitotenv.2019.07.102

Chandra, S., & Bhattacharya, J. (2019). Influence of temperature and duration of pyrolysis on the property heterogeneity of rice straw biochar and optimization of pyrolysis conditions for its application in soils. *Journal of Cleaner Production*, *215*, 1123–1139. https://doi.org/10.1016/j.jclepro.2019.01.079

Chen, Y., Yang, H., Wang, X., Zhang, S., & Chen, H. (2012). Biomass-based pyrolytic polygeneration system on cotton stalk pyrolysis: Influence of temperature. *Bioresource Technology*, *107*, 411–418. https://doi.org/10.1016/j.biortech.2011.10.074

Cui, X., Hao, H., Zhang, C., He, Z., & Yang, X. (2016). Capacity and mechanisms of ammonium and cadmium sorption on different wetland-plant derived biochars. *Science of the Total Environment*, *539*, 566–575. https://doi.org/10.1016/j.scitotenv.2015.09.022

de Jesus, J. H. F., da Cunha, G. C., Cardoso, E. M. C., Mangrich, A. S., & Romão, L. P. C. (2017). Evaluation of waste biomasses and their biochars for removal of polycyclic aromatic hydrocarbons. *Journal of Environmental Management*, *200*, 186–195. https://doi.org/10.1016/j.jenvman.2017.05.084

de Lange, W. J., Stafford, W. H. L., Forsyth, G. G., & le Maitre, D. C. (2012). Incorporating stakeholder preferences in the selection of technologies for using invasive alien plants as a bio-energy feedstock: Applying the analytical hierarchy process. *Journal of Environmental Management*, *99*, 76–83. https://doi.org/10.1016/j.jenvman.2012.01.014

Fernandes, M. J., Moreira, M. M., Paíga, P., Dias, D., Bernardo, M., Carvalho, M., … Delerue-Matos, C. (2019). Evaluation of the adsorption potential of biochars prepared from forest and agri-food wastes for the removal of fluoxetine. *Bioresource Technology*, *292*, 121973. https://doi.org/10.1016/j.biortech.2019.121973

Fidel, R. B., Laird, D. A., Thompson, M. L., & Lawrinenko, M. (2017). Characterization and quantification of biochar alkalinity. *Chemosphere*, *167*, 367–373. https://doi.org/10.1016/j.chemosphere.2016.09.151

Jiang, B., Lin, Y., & Mbog, J. C. (2018). Biochar derived from swine manure digestate and applied on the removals of heavy metals and antibiotics. *Bioresource Technology*, *270*, 603–611. https://doi.org/10.1016/j.biortech.2018.08.022

Keiluweit, M., Nico, P. S., Johnson, M. G., & Kleber, M. (2010). Dynamic molecular structure of plant biomass-derived black carbon (biochar). *Environmental Science & Technology*, *44*(4), 1247–1253. https://doi.org/10.1021/es9031419

Kong, L., Gao, Y., Zhou, Q., Zhao, X., & Sun, Z. (2018). Biochar accelerates PAHs biodegradation in petroleum-polluted soil by biostimulation strategy. *Journal of Hazardous Materials*, *343*, 276–284. https://doi.org/10.1016/j.jhazmat.2017.09.040

Leng, L., & Huang, H. (2018). An overview of the effect of pyrolysis process parameters on biochar stability. *Bioresource Technology*, *270*, 627–642. https://doi.org/10.1016/j.biortech.2018.09.030

Li, B. O., Liao, C.-H., Zhang, X.-D., Chen, H.-L., Wang, Q., Chen, Z.-Y., … Chen, J.-K. (2009). *Spartina alterniflora* invasions in the Yangtze River estuary, China: An overview of current status and ecosystem effects. *Ecological Engineering*, *35*(4), 511–520. https://doi.org/10.1016/j.ecoleng.2008.05.013

Li, H., Dong, X., da Silva, E. B., de Oliveira, L. M., Chen, Y., & Ma, L. Q. (2017). Mechanisms of metal sorption by biochars: Biochar characteristics and modifications. *Chemosphere*, *178*, 466–478. https://doi.org/10.1016/j.chemosphere.2017.03.072

Li, K., & Wang, X. (2009). Adsorptive removal of Pb(II) by activated carbon prepared from *Spartina alterniflora*: Equilibrium, kinetics and thermodynamics. *Bioresource Technology*, *100*(11), 2810–2815. https://doi.org/10.1016/j.biortech.2008.12.032

Li, M.-F., Li, X., Bian, J., Chen, C.-Z., Yu, Y.-T., & Sun, R.-C. (2015). Effect of temperature and holding time on bamboo torrefaction. *Biomass & Bioenergy*, *83*, 366–372. https://doi.org/10.1016/j.biombioe.2015.10.016

Li, M., Liu, Q., Guo, L., Zhang, Y., Lou, Z., Wang, Y., & Qian, G. (2013). Cu(II) removal from aqueous solution by *Spartina alterniflora* derived biochar. *Bioresource Technology*, *141*, 83–88. https://doi.org/10.1016/j.biortech.2012.12.096

Li, S., Harris, S., Anandhi, A., & Chen, G. (2019). Predicting biochar properties and functions based on feedstock and pyrolysis temperature: A review and data syntheses. *Journal of Cleaner Production*, *215*, 890–902. https://doi.org/10.1016/j.jclepro.2019.01.106

Liao, R., Gao, B., & Fang, J. (2013). Invasive plants as feedstock for biochar and bioenergy production. *Bioresource Technology*, *140*, 439–442. https://doi.org/10.1016/j.biortech.2013.04.117

Lu, J., & Zhang, Y. (2013). Spatial distribution of an invasive plant *Spartina alterniflora* and its potential as biofuels in China. *Ecological Engineering*, *52*, 175–181. https://doi.org/10.1016/j.ecoleng.2012.12.107

Mohan, D., Pittman, C. U., Bricka, M., Smith, F., Yancey, B., Mohammad, J., … Gong, H. (2007). Sorption of arsenic, cadmium, and lead by chars produced from fast pyrolysis of wood and bark during bio-oil production. *Journal of Colloid and Interface Science*, *310*(1), 57–73. https://doi.org/10.1016/j.jcis.2007.01.020

Moore, F., González, M.-E., Khan, N., Curaqueo, G., Sanchez-Monedero, M., Rilling, J., … Meier, S. (2018). Copper immobilization by biochar and microbial community abundance in metal-contaminated soils. *Science of the Total Environment*, *616–617*, 960–969. https://doi.org/10.1016/j.scitotenv.2017.10.223

Nie, C., Yang, X., Niazi, N. K., Xu, X., Wen, Y., Rinklebe, J., … Wang, H. (2018). Impact of sugarcane bagasse-derived biochar on heavy metal availability and microbial activity: A field study. *Chemosphere*, *200*, 274–282. https://doi.org/10.1016/j.chemosphere.2018.02.134

Oliveira, F. R., Patel, A. K., Jaisi, D. P., Adhikari, S., Lu, H., & Khanal, S. K. (2017). Environmental application of biochar: Current status and perspectives. *Bioresource Technology*, *246*, 110–122. https://doi.org/10.1016/j.biortech.2017.08.122

Pimentel, D. (2002). *Biological invasions economic and environmental cost of alien*. New York, NY: CRC Press.

Qin, F., Tang, B., Zhang, H., Shi, C., Zhou, W., Ding, L., & Qin, P. (2016). Potential use of *Spartina alterniflora* as forage for dairy cattle. *Ecological Engineering*, *92*, 173–180. https://doi.org/10.1016/j.ecoleng.2016.03.035

Qiu, Z., Zhou, X., Han, H., & Zhang, Q. (2018). Properties of *Spartina alterniflora* Loisel. derived-biochar and its effect on cadmium adsorption. *Journal of Agro-Environment Science*, *37*, 172–178.

Rajapaksha, A. U., Vithanage, M., Lim, J. E., Ahmed, M. B. M., Zhang, M., Lee, S. S., & Ok, Y. S. (2014). Invasive plant-derived biochar inhibits sulfamethazine uptake by lettuce in soil. *Chemosphere*, *111*, 500–504. https://doi.org/10.1016/j.chemosphere.2014.04.040

Raveendran, K., Ganesh, A., & Khilar, K. C. (1995). Influence of mineral matter on biomass pyrolysis characteristics. *Fuel*, *74*(12), 1812–1822. https://doi.org/10.1016/0016-2361(95)80013-8

Ronsse, F., van Hecke, S., Dickinson, D., & Prins, W. (2013). Production and characterization of slow pyrolysis biochar: Influence of feedstock type and pyrolysis conditions. *Global Change Biology Bioenergy*, *5*, 104–115. https://doi.org/10.1111/gcbb.12018

Shaaban, A., Se, S.-M., Dimin, M. F., Juoi, J. M., Husin, M. H. M., & Mitan, N. M. M. (2014). Influence of heating temperature and holding time on biochars derived from rubber wood sawdust via slow pyrolysis. *Journal of Analytical and Applied Pyrolysis*, *107*, 31–39. https://doi.org/10.1016/j.jaap.2014.01.021

Shen, Z., Hou, D., Jin, F., Shi, J., Fan, X., Tsang, D. C. W., & Alessi, D. S. (2019). Effect of production temperature on lead removal mechanisms by rice straw biochars. *Science of the Total Environment*, *655*, 751–758. https://doi.org/10.1016/j.scitotenv.2018.11.282

Shi, R., Li, J., Ni, N., & Xu, R. (2019). Understanding the biochar's role in ameliorating soil acidity. *Journal of Integrative Agriculture*, *18*(7), 1508–1517. https://doi.org/10.1016/S2095-3119(18)62148-3

Shimeta, J., Saint, L., Verspaandonk, E. R., Nugegoda, D., & Howe, S. (2016). Long-term ecological consequences of herbicide treatment to control the invasive grass, *Spartina anglica*, in an Australian saltmarsh. *Estuarine, Coastal and Shelf Science*, *176*, 58–66. https://doi.org/10.1016/j.ecss.2016.04.010

Shinogi, Y., & Kanri, Y. (2003). Pyrolysis of plant, animal and human waste: Physical and chemical characterization of the pyrolytic products. *Bioresource Technology*, *90*(3), 241–247. https://doi.org/10.1016/S0960-8524(03)00147-0

Simmons, M. T., Windhager, S., Power, P., Lott, J., Lyons, R. K., & Schwope, C. (2007). Selective and non-selective control of invasive plants: The short-term effects of growing-season prescribed fire, herbicide, and mowing in two texas prairies. *Restoration Ecology*, *15*(4), 662–669. https://doi.org/10.1111/j.1526-100X.2007.00278.x

Stefaniuk, M., Tsang, D. C. W., Ok, Y. S., & Oleszczuk, P. (2018). A field study of bioavailable polycyclic aromatic hydrocarbons (PAHs) in sewage sludge and biochar amended soils. *Journal of Hazardous Materials*, *349*, 27–34. https://doi.org/10.1016/j.jhazmat.2018.01.045

Tan, G., Sun, W., Xu, Y., Wang, H., & Xu, N. (2016). Sorption of mercury (II) and atrazine by biochar, modified biochars and biochar based activated carbon in aqueous solution. *Bioresource Technology*, *211*, 727–735. https://doi.org/10.1016/j.biortech.2016.03.147

Tang, L., Gao, Y., Wang, J., Wang, C., Li, B., Chen, J., & Zhao, B. (2009). Designing an effective clipping regime for controlling the invasive plant *Spartina alterniflora* in an estuarine salt marsh. *Ecological Engineering*, *35*(5), 874–881. https://doi.org/10.1016/j.ecoleng.2008.12.016

Tang, Y., Alam, M. S., Konhauser, K. O., Alessi, D. S., Xu, S., Tian, W., & Liu, Y. (2019). Influence of pyrolysis temperature on production of digested sludge biochar and its application for ammonium removal from municipal wastewater. *Journal of Cleaner Production*, *209*, 927–936. https://doi.org/10.1016/j.jclepro.2018.10.268

Taskin, E., Bueno, C. C., Allegretta, I., Terzano, R., Rosa, A. H., & Loffredo, E. (2019). Multianalytical characterization of biochar and hydrochar produced from waste biomasses for environmental and agricultural applications. *Chemosphere*, *233*, 422–430. https://doi.org/10.1016/j.chemosphere.2019.05.204

Vithanage, M., Rajapaksha, A. U., Tang, X., Thiele-Bruhn, S., Kim, K. H., Lee, S.-E., & Ok, Y. S. (2014). Sorption and transport of sulfamethazine in agricultural soils amended with invasive-plant-derived biochar. *Journal of Environmental Management*, *141*, 95–103. https://doi.org/10.1016/j.jenvman.2014.02.030

Vu, T. M., Trinh, V. T., Doan, D. P., Van, H. T., Nguyen, T. V., Vigneswaran, S., & Ngo, H. H. (2017). Removing ammonium from water using modified corncob-biochar. *Science of the Total Environment*, *579*, 612–619. https://doi.org/10.1016/j.scitotenv.2016.11.050

Wang, G., Qin, P., Wan, S., Zhou, W., Zai, X., & Yan, D. (2008). Ecological control and integral utilization of *Spartina alterniflora*. *Ecological Engineering*, *32*(3), 249–255. https://doi.org/10.1016/j.ecoleng.2007.11.014

Wang, X., Li, C., Li, Z., Yu, G., & Wang, Y. (2019). Effect of pyrolysis temperature on characteristics, chemical speciation and risk evaluation of heavy metals in biochar derived from textile dyeing sludge. *Ecotoxicology and Environmental Safety*, *168*, 45–52. https://doi.org/10.1016/j.ecoenv.2018.10.022

Wang, Y., & Liu, R. (2018). H_2O_2 treatment enhanced the heavy metals removal by manure biochar in aqueous solutions. *Science of the Total Environment*, *628–629*, 1139–1148. https://doi.org/10.1016/j.scitotenv.2018.02.137

Waqas, M., Khan, S., Qing, H., Reid, B. J., & Chao, C. (2014). The effects of sewage sludge and sewage sludge biochar on PAHs and potentially toxic element bioaccumulation in *Cucumis sativa* L. *Chemosphere*, *105*, 53–61. https://doi.org/10.1016/j.chemosphere.2013.11.064

Waryszak, P., Lenz, T. I., Leishman, M. R., & Downey, P. O. (2018). Herbicide effectiveness in controlling invasive plants under elevated CO_2: Sufficient evidence to rethink weeds management. *Journal of Environmental Management*, *226*, 400–407. https://doi.org/10.1016/j.jenvman.2018.08.050

Wei, X., Liu, D., Li, W., Liao, L., Wang, Z., Huang, W., & Huang, W. (2018). Biochar addition for accelerating bioleaching of heavy metals from swine manure and reserving the nutrients. *Science of the Total Environment*, *631–632*, 1553–1559. https://doi.org/10.1016/j.scitotenv.2018.03.140

Xu, X., Zhao, Y., Sima, J., Zhao, L., Mašek, O., & Cao, X. (2017). Indispensable role of biochar-inherent mineral constituents in its environmental applications: A review. *Bioresource Technology*, *241*, 887–899. https://doi.org/10.1016/j.biortech.2017.06.023

Yuan, J. H., Xu, R. K., & Zhang, H. (2011). The forms of alkalis in the biochar produced from crop residues at different temperatures. *Bioresource Technology*, *102*(3), 3488–3497. https://doi.org/10.1016/j.biortech.2010.11.018

Zhang, G., Guo, X., Zhu, Y., Han, Z., He, Q., & Zhang, F. (2017). Effect of biochar on the presence of nutrients and ryegrass growth in the soil from an abandoned indigenous coking site: The potential role of biochar in the revegetation of contaminated site. *Science of the Total Environment*, *601–602*, 469–477. https://doi.org/10.1016/j.scitotenv.2017.05.218

Zhang, J., Liu, J., & Liu, R. (2015). Effects of pyrolysis temperature and heating time on biochar obtained from the pyrolysis of straw and lignosulfonate. *Bioresource Technology*, *176*, 288–291. https://doi.org/10.1016/j.biortech.2014.11.011

Zhao, B., O'Connor, D., Zhang, J., Peng, T., Shen, Z., Tsang, D. C. W., & Hou, D. (2018). Effect of pyrolysis temperature, heating rate, and residence time on rapeseed stem derived biochar. *Journal of Cleaner Production*, *174*, 977–987. https://doi.org/10.1016/j.jclepro.2017.11.013

Zhao, S. X., Ta, N., & Wang, X. D. (2017). Effect of temperature on the structural and physicochemical properties of biochar with apple tree branches as feedstock material. *Energies*, *10*(9), 1293. https://doi.org/10.3390/en10091293

Zheng, S., Shao, D., Asaeda, T., Sun, T., Luo, S., & Cheng, M. (2016). Modeling the growth dynamics of *Spartina alterniflora* and the effects of its control measures. *Ecological Engineering*, *97*, 144–156. https://doi.org/10.1016/j.ecoleng.2016.09.006

Zhou, Z., Xu, Z., Feng, Q., Yao, D., Yu, J., Wang, D., … Zhong, M.-E. (2018). Effect of pyrolysis condition on the adsorption mechanism of lead, cadmium and copper on tobacco stem biochar. *Journal of Cleaner Production*, *187*, 996–1005. https://doi.org/10.1016/j.jclepro.2018.03.268

SUPPORTING INFORMATION

Additional supporting information may be found online in the Supporting Information section.

How to cite this article: Xia H, Kong W, Liu L, Li H, Lin K. Resource utilization conditions as biochar of an invasive plant *Spartina alterniflora* in coastal wetlands of China. *GCB Bioenergy*. 2020;12:636–647. https://doi.org/10.1111/gcbb.12717